Penicillin-binding proteins exhibit catalytic redundancy during asymmetric cell division in *Clostridioides difficile*

Shailab Shrestha[1,2†], Jules M. Dressler[1,2], Morgan E. McNellis[1,2], & Aimee Shen[1,*]

[1]Department of Molecular Biology and Microbiology, Tufts University School of Medicine, Boston, MA, USA.

[2]Program in Molecular Microbiology, Tufts University Graduate School of Biomedical Sciences, Boston, MA, USA.

[†] Current address: Department of Microbiology, Harvard Medical School, Boston, MA, USA.

*Address correspondence to aimee.shen@tufts.edu

Abstract

Peptidoglycan synthesis is an essential driver of bacterial growth and division. The final steps of this crucial process involve the activity of SEDS family glycosyltransferases that polymerize glycan strands and class B penicillin-binding protein (bPBP) transpeptidases that cross-link them. While most bacteria encode multiple bPBPs that perform specialized roles during specific cellular processes, some bPBPs can play redundant roles that are important for resistance against certain cell wall stresses. Our understanding of these compensatory mechanisms, however, remains incomplete. Endospore-forming bacteria typically encode multiple bPBPs that drive morphological changes required for sporulation. The sporulation-specific bPBP, SpoVD, is important for synthesizing the asymmetric division septum and spore cortex peptidoglycan during sporulation in the pathogen *Clostridioides difficile*. Although SpoVD catalytic activity is essential for cortex synthesis, we show that it is unexpectedly dispensable for SpoVD to mediate asymmetric division. The dispensability of SpoVD's catalytic activity requires the presence of its SEDS partner, SpoVE, and is facilitated by the catalytic activity of another sporulation-specific bPBP, PBP3. Our data further suggest that PBP3 interacts with components of the asymmetric division machinery, including SpoVD. These findings suggest a possible mechanism by which bPBPs can be functionally redundant in diverse bacteria and facilitate antibiotic resistance.

Introduction

Peptidoglycan (PG) synthesis is an essential driver of the morphological changes required for bacterial growth and division. The final steps of this crucial process include glycosyltransfer reactions that polymerize the glycan strands and transpeptidation reactions that crosslink the peptide sidechains between the strands (Egan et al., 2020; Rohs & Bernhardt, 2021). These enzymatic reactions require the activities of high-molecular-weight (HMW) Penicillin-binding proteins (PBPs) that are divided into two classes based on their catalytic ability: Class A PBPs (aPBP) are bifunctional enzymes capable of both glycosyltransferase and transpeptidase activities, while Class B PBPs are monofunctional transpeptidases (Goffin & Ghuysen, 1998; Sauvage et al., 2008). Since crosslinking of PG is essential in almost all bacteria, inhibiting PBP transpeptidase activity is typically lethal to bacterial cells. Consequently, beta-lactam antibiotics such as penicillin that inhibit PBPs by covalently bonding to the catalytic serine residue in their transpeptidase domain are some of the most successful and widely used antibiotics (Zapun et al., 2008). As such, identifying factors that confer resistance to beta-lactam antibiotics and determining their mechanism of action has been an area of significant interest.

One mechanism through which bacteria achieve resistance against beta-lactam antibiotics is by inducing the expression of PBPs with lowered binding affinities for specific beta-lactams. Most bacteria encode multiple PBPs that are specialized for specific cellular processes; some PBPs are essential, while others can be functionally redundant (Goffin & Ghuysen, 1998; Sauvage et al., 2008). Essential PBPs typically function as core components of highly conserved multiprotein complexes that drive cell wall synthesis during growth and division. The divisome is the essential complex responsible for driving septal PG synthesis through the activities of a bPBP transpeptidase that is partnered with a cognate glycosyltransferase, the latter of which is a member of the shape, elongation, division, and sporulation (SEDS) protein family (Cameron & Margolin, 2024; Rohs & Bernhardt, 2021; Taguchi et al., 2019). The elongasome is the multiprotein complex responsible for driving cell elongation in rod-shaped bacteria through the action of a distinct SEDS-bPBP pair (Emami et al., 2017; Meeske et al., 2015; Rohs & Bernhardt, 2021; Sjodt et al., 2020). Notably, these SEDS-bPBP pairs are highly specific because the bPBP acts as a selective allosteric activator of its cognate SEDS family glycosyltransferase activity (Shlosman et al., 2023; Sjodt et al., 2020).

Endospore-forming bacteria typically encode an additional SEDS-bPBP complex that is responsible for driving the morphological changes required for spore formation (Galperin et al., 2012, 2022; Shrestha et al., 2023; Tan & Ramamurthi, 2014). Sporulation begins with the formation of a polar division septum close to one cell pole in a process called asymmetric division. In *Bacillus subtilis*, asymmetric division is driven by the same SEDS-bPBP pair that mediates cell division during vegetative growth (Barák et al., 2019; Khanna et al., 2020). In contrast, we recently showed that the spore-forming pathogen *Clostridioides difficile* lacks a canonical division-associated SEDS-bPBP pair for driving septal PG synthesis and instead uses an aPBP as the major PG synthase during vegetative cell division (Shrestha et al., 2023). In further contrast with *B. subtilis,* the sporulation-specific SEDS-bPBP pair SpoVE-SpoVD is an important driver of septal PG synthesis during asymmetric division in *C. difficile*. Although the role of SpoVE-SpoVD function during asymmetric division may be restricted to *C. difficile* and other clostridial organisms, genes encoding SpoVE and SpoVD can be found in almost all spore formers (Galperin et al., 2012, 2022). In both *B. subtilis* and *C. difficile*, SpoVE and SpoVD are essential for the synthesis of the spore cortex, a thick layer of modified PG that surrounds and protects the spore core (Henriques et al., 1992; Yanouri et al., 1993; Daniel et al., 1994; Shrestha et al., 2023; Alabdali et al., 2021; Srikhanta et al., 2019). Thus, SpoVE and SpoVD are important for synthesizing PG during two distinct stages of spore formation in *C. difficile*.

While a previous study showed that SpoVD's catalytic activity is essential for spore formation in *C. difficile* (Alabdali et al., 2021), in this study, we surprisingly observe that SpoVD catalytic activity is largely dispensable for mediating asymmetric division despite being essential for synthesizing the cortex layer. Prior analyses of a catalytic mutant of a divisome-associated bPBP, PBP2b$_{Bs}$, in *B. subtilis* provide a possible mechanism for explaining this observation. In *B. subtilis*, the catalytic activity of PBP2b$_{Bs}$ is dispensable (Sassine et al., 2017) because a second bPBP, PBP3$_{Bs}$, can supply the transpeptidase activity during septal PG synthesis. Since the gene encoding PBP2b$_{Bs}$ is essential, presumably because the PBP2b$_{Bs}$ protein is required to allosterically activate the glycosyltransferase activity of its SEDS binding partner, FtsW, these observations highlight that PBP3$_{Bs}$ cannot complement all the roles fulfilled by the catalytically inactive PBP2b$_{Bs}$. Notably, PBP3$_{Bs}$ is also important for resistance against certain beta-lactams, since it has lower affinities for them compared to PBP2b$_{Bs}$ (Sassine et al., 2017). While these

observations highlight the importance of catalytic redundancies between PBPs, the molecular mechanisms behind this phenomenon remain unclear.

Here, we explore the role of SpoVD catalytic activity during asymmetric division in *C. difficile*. Our findings suggest that the ability of a catalytically inactive SpoVD to support septal PG synthesis during asymmetric division requires the presence of its SEDS partner SpoVE and is facilitated in part by another sporulation-specific bPBP, PBP3. Furthermore, we provide evidence suggesting that PBP3 interacts with components of the asymmetric division machinery, including SpoVD. These findings suggest a possible mechanism for how bPBPs in diverse bacteria can be functionally redundant and promote antibiotic resistance.

Results

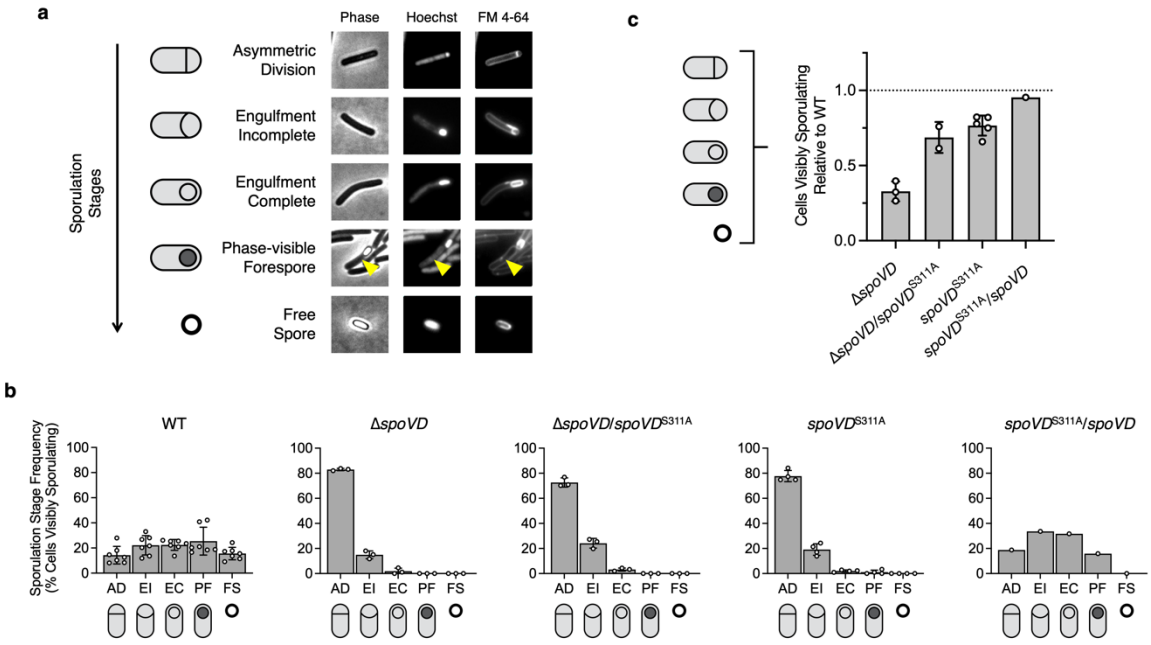

Fig. 1 | SpoVD catalytic activity is partially dispensable for its function during asymmetric division. **a** Cytological profile of individual cells representing each of the five morphological stages of sporulation as indicated. Representative phase-contrast and fluorescence micrographs are WT cells sampled from sporulation-inducing 70:30 plates after 18 of growth. The nucleoid was stained using Hoechst, and the cell membrane was stained using FM4-64. Cells undergoing asymmetric division (AD) have a flat polar septum; cells undergoing engulfment (EI) have a curved polar septum; cells that have completed engulfment (EC) exhibit bright-membrane staining around a fully engulfed forespore; phase-visible forespores (PF) are visible as phase-dark or phase-bright forespores associated with the mother cell (yellow arrow); mature free spores (FS) are observable as independent phase-bright particles. **b, c** Quantification of the cytological profiling of cells sampled from sporulation-inducing plates after 20-22 hours of growth. White circles

indicate data from each replicate, bars indicate average means, and error bars indicate standard deviation. >1,000 total cells and >100 visibly sporulating cells per sample. **b** shows the distribution of visibly sporulating cells among the indicated stages of sporulation. **c** shows the proportion of cells that complete and progress beyond asymmetric division, i.e., all visibly sporulating cells, as a percentage of the total cells profiled. Note that the data is normalized to WT (dotted line).

SpoVD catalytic mutant is defective in cortex synthesis but not in asymmetric division

Given that the catalytic activity of the division-specific bPBP in *B. subtilis* is not essential for its role in cell division (Sassine et al., 2017), we speculated that the catalytic activity of SpoVD might be similarly dispensable during asymmetric division in *C. difficile*. SpoVD retains the SXXK active-site motif that is highly conserved among bPBPs. To abolish the catalytic activity of SpoVD, we introduced an alanine substitution at the nucleophilic serine residue (SpoVD$_{S311A}$). Consistent with a prior study (Alabdali et al., 2021), *C. difficile* strains with a catalytically inactive SpoVD failed to produce heat-resistant spores (**Figure S1**). Importantly, this phenotype was observed when *spoVD*$_{S311A}$ was expressed from an ectopic chromosomal locus (Δ*spoVD*/*spoVD*$_{S311A}$) or the native locus (*spoVD*$_{S311A}$) (**Figure S1**). Furthermore, the levels of SpoVD present in these strains upon sporulation induction were found to be similar to wild-type (WT) by western blot analysis (**Figure S2**).

To further define the role of SpoVD catalytic activity during spore formation, we evaluated the ability of the SpoVD catalytic mutant strains to progress through the different morphological stages of sporulation by cytologically profiling sporulating cells (**Figure 1a**) (Nonejuie et al., 2013; Pogliano et al., 1999). Similar to the *spoVD* deletion strain, *spoVD* catalytic mutant strains failed to produce phase-visible spores, indicating that they have defects in cortex synthesis (**Figure 1b**). Furthermore, the distribution of sporulating cells among different stages was similar between the strains, with most cells being stalled at the asymmetric division stage and relatively few cells completing engulfment (**Figure 1b**). To specifically quantify the effects on asymmetric division, we calculated the proportion of cells that showed morphological signs of sporulation in the cytological profiling i.e., cells that progressed beyond asymmetric division, as a percentage of all cells. These analyses revealed that, relative to WT, Δ*spoVD*/*spoVD*^{S311A} and *spoVD*^{S311A} cells complete asymmetric division at significantly higher frequencies compared to Δ*spoVD* cells, with ~30% of Δ*spoVD* cells completing asymmetric division and ~70% of Δ*spoVD*/*spoVD*^{S311A} and *spoVD*^{S311A} cells completing asymmetric division

(**Figure 1c**). Since we have previously shown that the decreased frequency of Δ*spoVD* cells with visible signs of sporulation reflects a defect in asymmetric division rather than sporulation initiation (Shrestha et al., 2023), these results suggest that SpoVD function during asymmetric division is only partially dependent on its catalytic activity. Surprisingly, while we were able to complement the defects in asymmetric divison of the catalytic mutant strains by expressing a wild-type copy of *spoVD* from an ectopic locus (**Figure 1b, 1c**), this strain was unable to form mature phase-bright spores (**Figure S1, 1b**). This suggests that the catalytically inactive SpoVD has a dominant negative phenotype specifically for the defect in cortex synthesis.

The SpoVD catalytic mutant requires its SEDS partner, SpoVE

Since previous studies suggest that bPBPs are needed to allosterically activate the glycosyltransferase activity of their cognate SEDS family glycosyltransferases (Shlosman et al., 2023; Sjodt et al., 2020; Taguchi et al., 2019), we tested if the ability of SpoVD^{S311A} to support asymmetric division requires its SEDS partner SpoVE. To this end, we created a *spoVD*^{S311A}Δ*spoVE* strain by introducing the catalytic mutant variant of *spoVD* into the native locus of a Δ*spoVD*Δ*spoVE* strain. As expected, this strain failed to form heat-resistant spores (**Figure 2**). Cytological profiling of sporulating cells revealed that *spoVD*^{S311A}Δ*spoVE* cells complete and progress beyond asymmetric division at a significantly lower frequency (~25%) than WT or *spoVD*^{S311A} cells (100% and ~75%, respectively). Thus, the phenotype of *spoVD*^{S311A}Δ*spoVE* cells is similar to that of Δ*spoVD* and Δ*spoVE* cells (**Figure 2**). Since we previously showed that SpoVD levels are unaffected by loss of SpoVE (Shrestha et al., 2023), we conclude that the function of SpoVD^{S311A} during asymmetric division requires SpoVE.

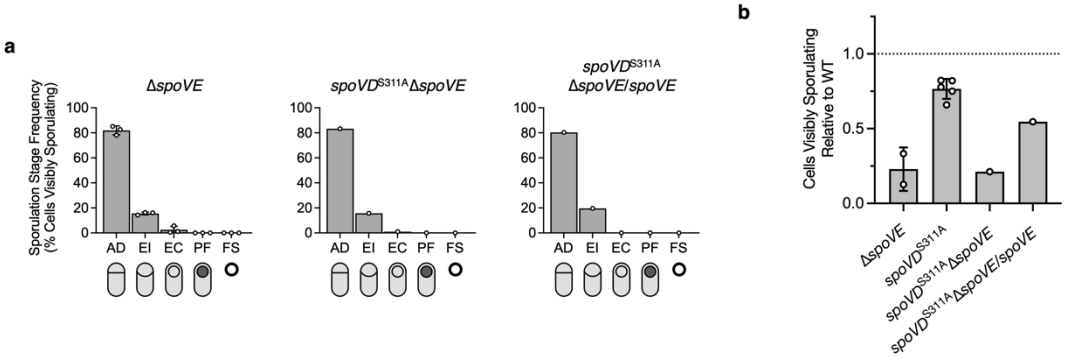

Fig. 2 | The catalytically inactive SpoVD requires its SEDS partner, SpoVE, to facilitate asymmetric division. a, b Quantification of the cytological profiling of cells sampled from sporulation-inducing plates after 20-22 hours of growth. White circles indicate data from each replicate, bars indicate the average mean, and error bars indicate standard deviation. >1,000 total cells and >100 visibly sporulating cells per

sample. **a** shows the distribution of visibly sporulating cells among the indicated stages of sporulation. See Figure 1b for the distribution of WT cells. AD, Asymmetric Division; EI, Engulfment Initiated; EC, Engulfment Completed; PF, Phase bright/dark Forespore; FS, Free Spore. **b** shows the proportion of cells that complete and progress beyond asymmetric division, i.e., all visibly sporulating cells, as a percentage of the total cells profiled. Note that the data is normalized to WT (dotted line).

An additional non-essential bPBP, PBP3, is involved in sporulation

Next, we wondered if *C. difficile* encodes an additional sporulation-specific bPBP that can cross-link septal PG synthesis in the absence of SpoVD catalytic activity similar to the functional redundancy observed between division-specific bPBPs in *B. subtilis* (Sassine et al., 2017). Most *C. difficile* strains encode three bPBPs (Isidro et al., 2017, 2018): one sole essential bPBP, PBP2, which primarily functions during cell elongation, and two other bPBPs, SpoVD and PBP3, which are dispensable for vegetative growth (Shrestha et al., 2023). PBP3 is a close homolog of SpoVD containing a similar domain composition apart from the C-terminal PASTA (PBP And Serine/Threonine kinase Associated) domain carried by SpoVD (**Figure 3a**). Both PBP3 and SpoVD have an N-terminal transmembrane section followed by PBP dimerization and transpeptidase domains.

We considered PBP3 to be a likely candidate for providing functional redundancy to SpoVD during asymmetric division for several reasons. First, previous studies suggest that the expression of *pbp3* (locus *cd630_12290* in the strain used in this study) is upregulated at the onset of sporulation in a manner similar to *spoVD* expression (Fimlaid et al., 2013; Saujet et al., 2013). Second, we previously showed that individual deletions of *spoVD* or *pbp3* do not affect the growth rate of vegetative cells, suggesting that SpoVD and PBP3 play sporulation-specific roles (Shrestha et al., 2023). This agrees with our western blot analysis showing that SpoVD and PBP3 are produced under sporulation-inducing conditions in a manner dependent on the presence of the master transcriptional regulator of sporulation, Spo0A **(Figure 3).** Taken together with prior transcriptomic studies (Fimlaid et al., 2013; Saujet et al., 2013), which similarly show Spo0A-dependent induction of *pbp3* and *spoVD* transcription, these observations demonstrate that both proteins are produced prior to asymmetric division. Furthermore, the Δ*pbp3* strain forms heat-resistant spores ~2-fold less efficiently than WT, a modest defect that can be complemented by expressing *pbp3* from an ectopic chromosomal locus (**Figure 3c**). This result is consistent with a prior transposon mutagenesis screen, which identified *pbp3* to be important

for sporulation (Dembek et al., 2015). Since phase-contrast microscopy of sporulating cells revealed that the Δ*pbp3* mutant forms phase-bright forespores and free spores, and thus capable of assembling the spore cortex, our data indicate that PBP3 is dispensable for this process unlike SpoVD (**Figure 3d**). These results suggest that PBP3 is a sporulation-specific factor that is involved in, but not essential for, the formation of mature spores in *C. difficile*.

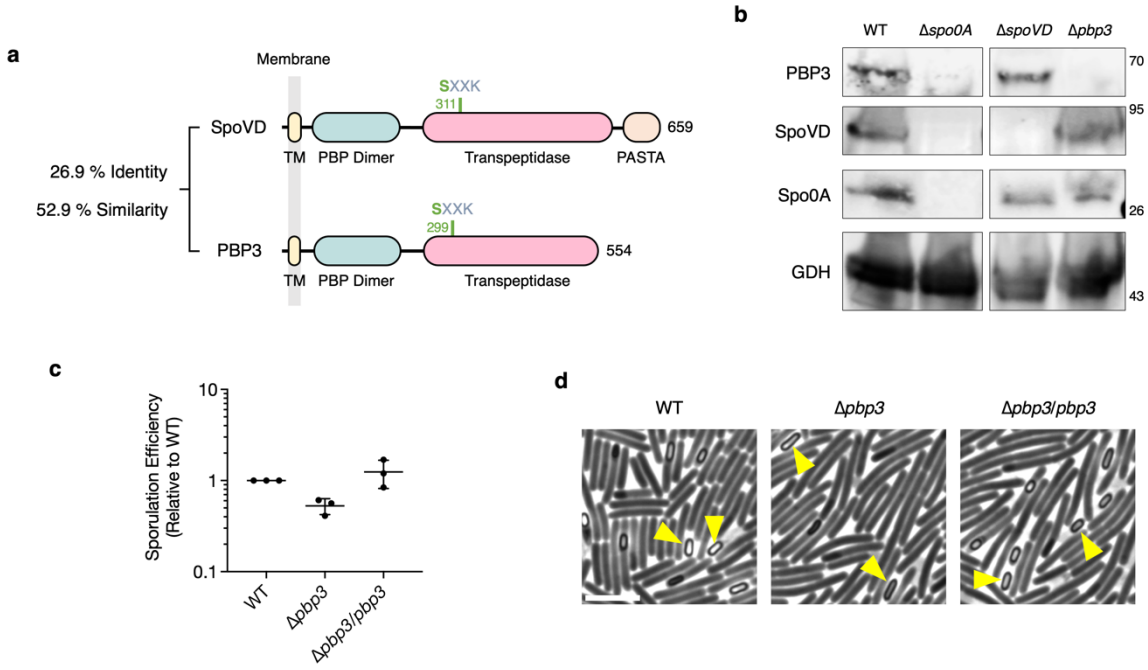

Fig. 3 | PBP3 is a sporulation-specific bPBP involved in spore formation. a Protein schematic comparing SpoVD and PBP3. Functional domains and catalytic sites were predicted using HMMER. TM, transmembrane domain; PASTA, penicillin-binding protein and serine/threonine kinase-associated domain. **b** Western blot showing the levels of the SpoVD, PBP3, Spo0A, and GDH in WT, Δ*spo0A*, Δ*spo0A*, and Δ*pbp3* cells sampled from sporulation-inducing plates after ~20 hours of growth. SpoVD and PBP3 are not detected in the Δ*spo0A* strain, which cannot initiate sporulation. Levels of the constitutively produced glutamate dehydrogenase (GDH) are shown as a control. **c** Efficiency of heat-resistant spore formation (sporulation efficiency) of the *pbp3* mutant and complemented strains relative to WT. Means with standard deviation are indicated. Cells were collected from sporulation-inducing 70:30 plates ~20-22 hours after inoculation. Data from three independent experiments. **d** Representative phase-contrast micrographs of WT, *pbp3* mutant, and complemented cells collected from sporulation-inducing 70:30 plates after ~20 hours of growth. Examples of phase-bright spores are indicated by yellow arrows. Scale bar, 5 μm.

PBP3 can partially substitute for the loss of SpoVD catalytic activity during asymmetric division

To test if PBP3 provides redundancy to SpoVD catalytic activity during asymmetric division, we analyzed the ability of Δ*pbp3* cells to complete asymmetric division in the context of WT and

catalytically inactive SpoVD variants. Cells lacking PBP3 completed asymmetric division at WT levels in the presence of WT SpoVD (**Figure 4b**). The distribution of sporulating Δ*pbp3* cells among the different sporulation stages was also similar to WT (**Figure 4a**). Importantly, in a SpoVD catalytic mutant background, cells lacking PBP3 completed asymmetric division at a lower rate when compared to WT or *spoVD*^{S311A} cells (**Figure 4b**). However, the proportion of *spoVD*^{S311A}Δ*pbp3* cells that complete asymmetric division was higher compared to Δ*spoVD* cells (**Figure 4b**), suggesting that PBP3 transpeptidase only partially accounts for the ability of the catalytically dead SpoVD to support asymmetric division. To establish if this partial redundancy requires the transpeptidase activity of PBP3, we introduced *pbp3*^{S299A}, which encodes a catalytically inactive PBP3 in an ectopic chromosomal locus of a *spoVD*^{S311A} Δ*pbp3* strain. Cytological profiling of the *spoVD*^{S311A} Δ*pbp3*/*pbp3*^{S299A} strain revealed that these cells complete asymmetric division at a similar rate to the *spoVD*^{S311A} strain (**Figure 4**). Hence, our data suggest that the transpeptidase activity of PBP3 provides partial functional redundancy to SpoVD catalytic activity specifically during asymmetric division.

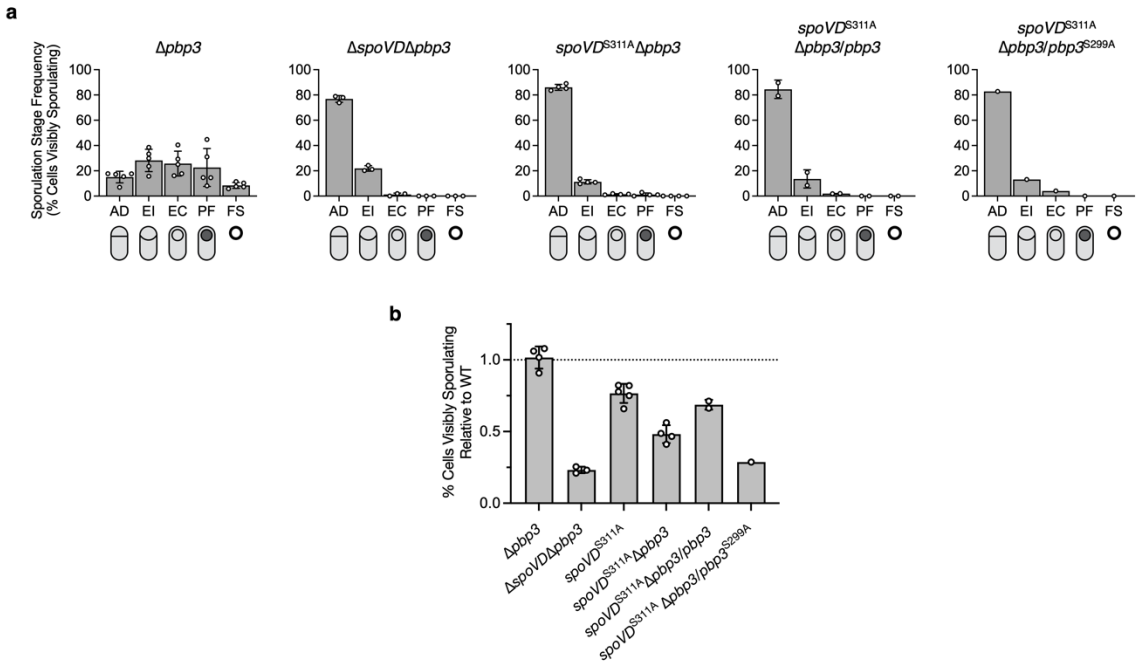

Fig. 4 | PBP3 catalytic activity plays a partially redundant role to SpoVD catalytic activity during asymmetric division. a, b Quantification of the cytological profiling of cells sampled from sporulation-inducing plates after 20-22 hours of growth. White circles indicate data from each replicate, bars indicate average means, and error bars indicate standard deviation. >1,000 total cells and >100 visibly sporulating cells per sample. **a** shows the distribution of visibly sporulating cells among the indicated stages of

sporulation. See **Figure 1b** for the distribution of WT cells. AD, Asymmetric Division; EI, Engulfment Initiated; EC, Engulfment Completed; PF, Phase bright/dark Forespore; FS, Free Spore. **b** shows the proportion of cells that complete and progress beyond asymmetric division, i.e., all visibly sporulating cells, as a percentage of the total cells profiled. Note that the data is normalized to WT (dotted line).

PBP3 may interact with PG-synthesizing enzymes and components of the polar divisome

Our previous study suggests that SpoVD likely functions as part of the polar divisome to synthesize septal PG during asymmetric division (Shrestha et al., 2023). The partial redundancy between PBP3 and SpoVD catalytic activities during asymmetric division observed here suggests that PBP3 might be recruited to this machinery during this process. To test whether PBP3 interacts with polar divisome, we conducted bacterial two-hybrid assays to probe pairwise interactions between PBP3 and various components of this complex. In addition to SpoVD and SpoVE, we explored interactions with three additional proteins, FtsL, FtsQ, and FtsB (also known as FtsL, DivIB, and DivIC in some Firmicutes), which form a highly-conserved divisome sub-complex that regulates PG synthase activity during cell division in other bacteria (Levin & Losick, 1994; Daniel et al., 1998; Katis & Wake, 1999; Tsang & Bernhardt, 2015; Marmont & Bernhardt, 2020; Shrestha et al., 2023). Our data suggests that PBP3 can interact with various components of the polar divisome, including SpoVD, SpoVE, and FtsQ (**Figure 5a**). As controls, we also probed interactions between PBP3 and all other PBP and SEDS-family proteins encoded by *C. difficile*. Surprisingly, our analysis indicates that PBP3 also interacts with PBP2 and PBP1 (**Figure 5a**), which primarily function during vegetative cell elongation and division, respectively, but likely also play important roles during spore formation. Although surprising, this suggests that PBP3 may be able to supplement the transpeptidation activities of other PBPs in *C. difficile* during spore formation. Overall, our data implies that PBP3 is recruited to the polar divisome complex through direct interactions with its components (**Figure 5b**).

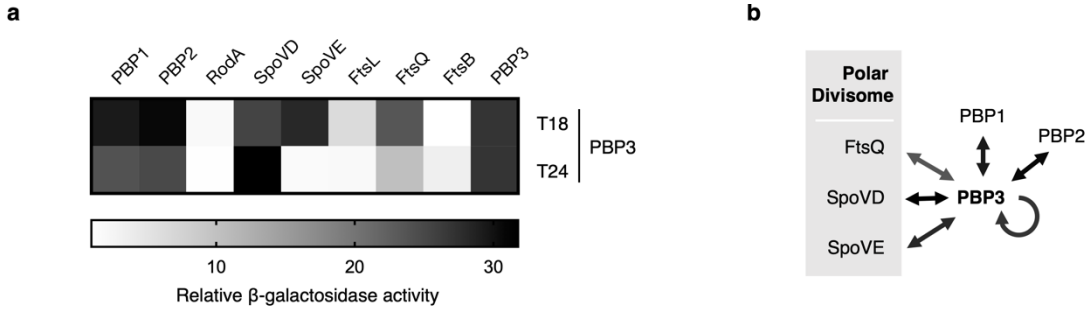

Fig. 5 | PBP3 interacts with multiple components of the polar divisome. a Bacterial two-hybrid analysis of interactions between PBP3 and other PG synthases or components of the polar divisome. The

β-galactosidase activity was normalized to the negative control. N-terminal T18 or T24 fusion to PBP3 was paired with reciprocal N-terminal fusions to the indicated proteins. Data from three technical replicates. **B** The schematic shows detected interactions from (a) where arrows are colored according to the amount of maximum β-galactosidase activity detected. Components of the predicted polar divisome are indicated.

Endospore-forming bacteria typically encode multiple additional bPBPs compared to non-sporulating bacteria

Since *B. subtilis* also encodes multiple sporulation-specific class B PBPs, we wondered whether functional redundancies between sporulation-specific bPBPs might be more broadly conserved in endospore-forming bacteria. To this end, we compared the numbers of SEDS and bPBP enzymes encoded in the genomes of non-sporulating and sporulating Firmicutes, the sole bacterial phyla with endospore-forming members. Our analyses revealed that sporulating bacteria typically encode a higher number of bPBPs compared to non-sporulating bacteria (**Figure 6**). In sporulating organisms, the number of encoded bPBPs often exceeds the number of encoded SEDS (214/328; 65%), while only a small minority encode more SEDS proteins than bPBPs (20/328; 6%). Furthermore, a higher percentage of non-sporulating organisms encode equal numbers of SEDS and bPBP genes (80%). These observations are consistent with the prevalence of additional sporulation-specific PG synthases in spore formers and suggest that redundancy in bPBP activity is likely widespread in these organisms.

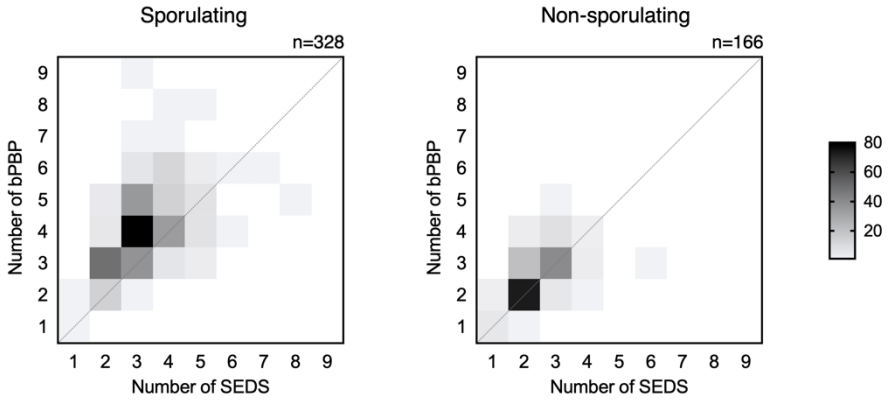

Fig. 6 | Prevalence of bPBP and SEDS enzymes in Firmicutes. Heatmaps showing the distribution of class B penicillin-binding protein (bPBP) and SEDS protein numbers encoded in the genomes of sporulating (n=328) and non-sporulating (n=166) Firmicutes organisms. Sporulation ability was inferred by the presence of broadly conserved sporulation-specific genes *spo0A* and *spoIIE* in the genome. The dataset is composed of 494 diverse Firmicutes organisms as reported in Shrestha *et al*., 2023.

Discussion

While most bacteria encode multiple bPBPs that perform specialized roles during specific cellular processes, some bPBPs can play redundant roles that are important for resistance against environmental stresses. Our understanding of these compensatory mechanisms and their prevalence, however, remains incomplete. Here, we reveal that the catalytic activity of SpoVD in *C. difficile* is partially dispensable for its function during the synthesis of the polar septum (**Figure 1)**. Furthermore, we demonstrate that a previously uncharacterized sporulation-specific bPBP, PBP3, is important for this dispensability since it can partially substitute for SpoVD's catalytic activity during asymmetric division (**Figures 3, 4**). Finally, our data suggests that PBP3 likely functions as a part of the polar divisome, which mediates asymmetric division, via direct interactions with its components (**Figure 5**).

Functional redundancies between PBPs have important implications for cellular adaptation to environmental stresses and resistance against antibiotics targeting PG transpeptidation. Redundancies between aPBPs have been described in *Escherichia coli* (Mueller et al., 2019), *B. subtilis,* and *Streptococcus pneumoniae* (Mitchell et al., 2023), where distinct aPBPs are specialized to respond to changes in environmental pH but can also play redundant roles in certain conditions. Similarly, niche specialization of different bPBPs was observed in *Salmonella enterica*, which encodes two division-specific and two elongation-specific bPBPs that are functionally specialized for extracellular or intracellular conditions (Castanheira et al., 2017, 2020). Furthermore, as described above, functional redundancy in bPBP activities during cell division in *B. subtilis* lowers its sensitivity to certain β-lactams (Sassine et al., 2017). Given that different bPBPs have distinct binding affinities to β-lactams, it is thought that typically dispensable bPBPs can facilitate resistance by providing transpeptidation activity with an inherently low affinity to the inhibitor when an essential bPBP is targeted. This is supported by studies in methicillin-resistant *Staphylococcus aureus* (MRSA), where strains that have acquired an additional low-affinity bPBP display lower sensitivity to certain β-lactams (Hartman & Tomasz, 1984; Wielders et al., 2002). Similarly, a typically non-essential *Enterococcus faecalis* bPBP with low reactivity to cephalosporins provides functional redundancy to the primary division-associated bPBP during cephalosporin treatment (Djorić et al., 2020; Nelson et al., 2024).

While the molecular mechanisms enabling redundancies between bPBPs remain unclear, these observations suggest a few different possibilities. In the case of *S. enterica*, the two division-specific bPBPs appear to function independently since neither bPBP requires the presence of the other to function in their respective niche (Castanheira et al., 2017). In contrast, the functional redundancy reported between PBP3$_{Bs}$ and PBP2b$_{Bs}$ in *B. subtilis* when the catalytic activity of the primary division-specific bPBP, PBP2b$_{Bs}$ is inactivated depends on the presence of the catatlytically inactivated PBP2b$_{Bs}$ protein (Sassine et al., 2017). Since SEDS-bPBP pairs are thought to be comprised of cognate partners whose activities are coordinated by and require their interaction (Shlosman et al., 2023; Sjodt et al., 2020; Taguchi et al., 2019), it is likely that the requirement of PBP2b$_{Bs}$ is dictated by the structural role it plays in interacting with and stimulating the glycosyltransferase activity of the division-specific SEDS protein. This is consistent with an *in vitro* study, which showed that a catalytically inactive form of a bPBP can support PG polymerization by its SEDS partner (Taguchi et al., 2019). Furthermore, the redundancy observed in *E. faecalis* is suggested to require direct interaction between the two bPBPs within the larger divisome complex (Nelson et al., 2024). In contrast, since the two division-specific bPBPs in *S. enterica* can function independently from one another, it is possible that either enzyme can interact with the division-specific SEDS glycosyltransferase (Castanheira et al., 2017).

Since the activity of *C. difficile* PBP3 during asymmetric division requires the presence of SpoVD (**Figure 1**), redundancy between these sporulation-specific bPBPs is analogous to the catalytic redundancy observed between division-specific bPBPs in *B. subtilis*. We speculate that the requirement for SpoVD, even when catalytically inactive, is due to SpoVD's function in allosterically activating SpoVE activity. In addition, SpoVD may play a crucial role in the formation and function of the polar divisome complex. Importantly, our results show that PBP3 can interact with different members of the polar divisome, suggesting it may be recruited to this complex during asymmetric division. The active recruitment of functionally redundant bPBPs to the divisome is consistent with the finding that septal PG synthesis is a highly controlled process involving various localization and regulatory mechanisms (Egan et al., 2020). Moreover, since functional redundancies appear to be constrained to distinct bPBP pairs and specialized for specific cellular processes, it is unlikely that a functionally redundant bPBP functions independently. Due to the requirement for SpoVD, we speculate that PBP3 is likely recruited as

an additional factor rather than replacing SpoVD in the polar divisome complex. However, confirmation and characterization of the mechanisms and factors facilitating this recruitment require further study. Since bacterial two-hybrid assays only probe pairwise interactions in a non-native system, it will be important to define these interactions in the native context, including all components of the polar divisome.

It remains unclear why SpoVD catalytic activity is largely dispensable for during asymmetric division but essential for cortex synthesis. It is possible that cortex synthesis involves SpoVE-SpoVD to function as part of a larger PG synthetic complex, similar to the divisome and elongasome. Since SpoVE-SpoVD function during this process requires their specific localization to the forespore, it is likely that other factors are involved in their regulation. It is, therefore, possible that the inability of PBP3 to functionally compensate for the loss of SpoVD catalytic activity during cortex synthesis results from its decreased affinity for these unknown factors. Another possibility is that the amount of crosslinking required is higher than PBP3 is able to supplement during this process. This is consistent with our finding that an ectopically expressed *spoVD* is unable to alleviate the cortex synthesis defect observed upon introducing the catalytic mutation in the native copy of *spoVD*. Thus, more research is required to define the factors and mechanisms regulating SpoVE-SpoVD activity during cortex synthesis.

Finally, redundancy in bPBP activity is likely widespread among spore-forming bacteria based on our finding that they typically encode multiple additional bPBPs, the number of which often exceeds the number of SEDS glycosyltransferases encoded in the genome (**Figure 6**). Defining specialized roles or redundancies between these enzymes requires further study and may have important implications of the ability of these organisms to respond to environmental and antibiotic stress. Interestingly, while most *C. difficile* strains carry five distinct HMW PBPs, a study characterizing clinical strains identified an additional bPBP encoded by *Clostridium difficile* ribotype 017 isolates (Isidro et al., 2017, 2018). Some of these isolates have a lower sensitivity to the beta-lactam imipenem and carry mutations in the transpeptidase catalytic sites of the division-associated PBP1 and elongation-associated PBP2. The additional bPBP encoded by these strains, therefore, may additionally contribute to imipenem resistance by providing functional redundancy to these enzymes or SpoVD, recapitulating the scenario observed in MRSA strains. Taken together with our findings, these observations highlight the need to define

functional redundancies between PBPs in *C. difficile* and their possible roles in driving antibiotic resistance of this important pathogen.

Methods

C. difficile strain construction and growth conditions

All *C. difficile* strains are derived from the 630Δ*erm* strain. Deletion and complementation strains were constructed in a Δ*pyrE* background strain using *pyrE*-based allele-coupled exchange as previously described (Ng et al., 2013). All strains used in the study are reported in Table 1. Strains were grown at 37°C under anaerobic conditions using a gas mixture containing 85% N_2, 5% CO_2, and 10% H_2.

E. coli strain constructions

Table 2 lists all plasmids used in the study, with links to plasmid maps containing all primer sequences used for cloning. Plasmids were cloned via Gibson assembly, and cloned plasmids were transformed into *E. coli* (DH5α or XL1-Blue strains). All plasmids were confirmed by sequencing the inserted region. Confirmed plasmids were transformed into the *E. coli* HB101(pRK24) strain for conjugation with *C. difficile* when needed. All *E. coli* HB101 strains used for conjugation are also listed in Table 2.

Plate-based sporulation assays

For assays requiring sporulating cells, cultures were grown to early stationary phase, back-diluted >25-fold into BHIS, and grown until they reached exponential phase (OD_{600} between 0.35 and 0.75). 120 µL of exponentially growing cells were spread onto 70:30 (70% SMC media and 30% BHIS media) agar plates (40 mL media per plate). After 18-22 hours of growth, sporulating cells were collected into phosphate-buffered saline (PBS), and sporulation levels were visualized by phase-contrast microscopy as previously described (Pishdadian et al., 2015).

Heat resistance assay

Heat-resistant spore formation was measured 20-22 hours after sporulation induction on 70:30 agar plates by resuspending sporulating cells in PBS, dividing the sample into two, heat-treating one of the samples at 60˚C for ~30 min, and comparing the colony-forming units (CFUs) in the untreated sample to the heat-treated sample (Fimlaid et al., 2015). Heat-resistance efficiencies

represent the average ratio of heat-resistant CFUs to total CFUs for a given strain relative to the average ratio for the wild-type strain.

Western blot analysis

Samples were collected 18-22 hours after sporulation induction on 70:30 agar plates and processed for immunoblotting. Sample processing involved multiple freeze-thaws in PBS followed by the addition of EBB buffer (9 M urea, 2 M thiourea, 4% SDS, 2 mM b-mercaptoethanol), boiling, pelleting, resuspension, and boiling again before loading on a gel. All proteins were resolved using 4–15% precast polyacrylamide gels (Bio-Rad) and transferred to polyvinylidene difluoride membranes, which were subsequently probed with rabbit (anti-PBP3 and anti-SpoVD (Shrestha et al., 2023); both at 1:1,000 dilution), mouse (anti-Spo0A (Fimlaid et al., 2013) at 1:1,000 dilution) and chicken (anti-GDH at 1:5,000 dilution) polyclonal primary antibodies, and anti-rabbit (IR800 or IR680), anti-mouse (IR680) and anti-chicken (IR800) secondary antibodies (LI-COR Biosciences, 1:20,000 dilution). Blots were imaged using a LiCor Odyssey CLx imaging system. The results shown are representative of multiple experiments.

Bacterial two-hybrid analyses

Bacterial adenylate cyclase two-hybrid (BACTH) assays were conducted as previously described (Karimova et al., 1998) using *E. coli* BTH101 cells. Briefly, BTH101 cells were transformed with 100 ng of each plasmid and plated on LB agar plates supplemented with 50 µg/ml kanamycin, 100 µg/ml Ampicillin, and 0.5 mM isopropyl β-D-thiogalactopyranoside (IPTG). Plates were incubated for 64-68 hours at 30°C, and β-galactosidase activity was quantified in Miller units as previously detailed (Dahlstrom et al., 2015). The β-galactosidase activity of cells transformed with the empty pUT18C and pKT25 vectors was used as a negative control for normalization.

Cell labeling and microscopy

Fluorescence microscopy was performed on sporulating cells using Hoechst 33342 (Molecular Probes; 15 µg/mL) and FM4-64 (Invitrogen; 1 µg/mL) to stain nucleoid and membrane, respectively. All samples for a given experiment were imaged from a single agar pad (1.5% low-melting point agarose in PBS).

Phase-contrast images in **Figure 3** were obtained using a Zeiss Axioskop upright microscope with a 100× Plan-NEOFLUAR oil-immersion phase-contrast objective and a Hamamatsu C4742-95 Orca 100 CCD Camera. All other phase-contrast and fluorescence images were acquired using a Leica DMi8 inverted microscope with a 63× 1.4 NA Plan Apochromat oil-immersion phase-contrast objective, a high precision motorized stage (Pecon), and an incubator (Pecon) set at 37˚C. Excitation light was generated by a Lumencor Spectra-X multi-LED light source with integrated excitation filters. An XLED-QP quadruple-band dichroic beam-splitter (Leica) was used (transmission: 415, 470, 570, and 660 nm) with an external filter wheel for all fluorescent channels. FM4-464 was excited at 550/38 nm and emitted light was filtered using a 705/72 nm emission filter (Leica); Hoechst was excited at 395/40 nm and emitted light was filtered using a 440/40 nm emission filter (Leica). Emitted and transmitted light was detected using a Leica DFC 9000 GTC sCMOS camera. 1 to 2 µm z-stacks were taken when needed with 0.21 µm z-slices.

Images were acquired and exported using the LASX software without further processing. After export, images were processed using Fiji (Schindelin et al., 2012) to remove out-of-focus regions, and the best-focused z-planes for all channels were manually selected. Image scaling was adjusted to improve brightness and contrast for display and was applied equally to all images shown in a single panel. Visualization of quantified data and any associated statistical tests were performed using Prism 10 (GraphPad Software, San Diego, CA, USA).

Acknowledgments

We acknowledge the University of Vermont Microscopy Imaging Core for processing the samples and acquiring the images for all Transmission Electron Microscopy analyses. We are grateful to members of the Shen lab for helpful discussions and feedback on the project. The National Institute of Allergy and Infectious Diseases grant R01 AI122232 (to A.S.) and Burroughs Wellcome Fund for Investigators in Pathogenesis Award (to A.S.) provided funding for this work.

Author Contributions

S.S. and A.S. conceived the study. S.S., J.M.D., and M.M. performed and analyzed experiments. A.S. supervised the study. S.S. wrote the manuscript with input from the other authors. All authors reviewed and approved the manuscript.

References

Alabdali, Y. A. J., Oatley, P., Kirk, J. A., & Fagan, R. P. (2021). A cortex-specific penicillin-binding protein contributes to heat resistance in *Clostridioides difficile* spores. *Anaerobe*, *70*, 102379. https://doi.org/10.1016/j.anaerobe.2021.102379

Barák, I., Muchová, K., & Labajová, N. (2019). Asymmetric cell division during *Bacillus subtilis* sporulation. *Future Microbiology*, *14*(4), 353–363. https://doi.org/10.2217/fmb-2018-0338

Cameron, T. A., & Margolin, W. (2024). Insights into the assembly and regulation of the bacterial divisome. *Nature Reviews Microbiology*, *22*(1), 33–45. https://doi.org/10.1038/s41579-023-00942-x

Castanheira, S., Cestero, J. J., Rico-Pérez, G., García, P., Cava, F., Ayala, J. A., Pucciarelli, M. G., & García-del Portillo, F. (2017). A Specialized Peptidoglycan Synthase Promotes *Salmonella* Cell Division inside Host Cells. *mBio*, *8*(6), e01685-17. https://doi.org/10.1128/mBio.01685-17

Castanheira, S., López-Escarpa, D., Pucciarelli, M. G., Cestero, J. J., Baquero, F., & García-del Portillo, F. (2020). An alternative penicillin-binding protein involved in *Salmonella* relapses following ceftriaxone therapy. *eBioMedicine*, *55*, 102771. https://doi.org/10.1016/j.ebiom.2020.102771

Dahlstrom, K. M., Giglio, K. M., Collins, A. J., Sondermann, H., & O'Toole, G. A. (2015). Contribution of Physical Interactions to Signaling Specificity between a Diguanylate Cyclase and Its Effector. *mBio*, *6*(6), 10.1128/mbio.01978-15. https://doi.org/10.1128/mbio.01978-15

Daniel, R. A., Drake, S., Buchanan, C. E., Scholle, R., & Errington, J. (1994). The *Bacillus subtilis spoVD* gene encodes a mother-cell-specific penicillin-binding protein required for spore morphogenesis. *Journal of Molecular Biology*, *235*(1), 209–220. https://doi.org/10.1016/S0022-2836(05)80027-0

Daniel, R. A., Harry, E. J., Katis, V. L., Wake, R. G., & Errington, J. (1998). Characterization of the essential cell division gene *ftsL*(*yIID*) of *Bacillus subtilis* and its role in the assembly of the division apparatus. *Molecular Microbiology*, *29*(2), 593–604. https://doi.org/10.1046/j.1365-2958.1998.00954.x

524 Dembek, M., Barquist, L., Boinett, C. J., Cain, A. K., Mayho, M., Lawley, T. D., Fairweather, N.
525 F., & Fagan, R. P. (2015). High-throughput analysis of gene essentiality and sporulation
526 in *Clostridium difficile*. *mBio*, *6*(2), e02383. https://doi.org/10.1128/mBio.02383-14
527 Djorić, D., Little, J. L., & Kristich, C. J. (2020). Multiple Low-Reactivity Class B Penicillin-
528 Binding Proteins Are Required for Cephalosporin Resistance in Enterococci.
529 *Antimicrobial Agents and Chemotherapy*, *64*(4), 10.1128/aac.02273-19.
530 https://doi.org/10.1128/aac.02273-19
531 Egan, A. J. F., Errington, J., & Vollmer, W. (2020). Regulation of peptidoglycan synthesis and
532 remodelling. *Nature Reviews. Microbiology*, *18*(8), 446–460.
533 https://doi.org/10.1038/s41579-020-0366-3
534 Emami, K., Guyet, A., Kawai, Y., Devi, J., Wu, L. J., Allenby, N., Daniel, R. A., & Errington, J.
535 (2017). RodA as the missing glycosyltransferase in *Bacillus subtilis* and antibiotic
536 discovery for the peptidoglycan polymerase pathway. *Nature Microbiology*, *2*, 16253.
537 https://doi.org/10.1038/nmicrobiol.2016.253
538 Fimlaid, K. A., Bond, J. P., Schutz, K. C., Putnam, E. E., Leung, J. M., Lawley, T. D., & Shen, A.
539 (2013). Global Analysis of the Sporulation Pathway of *Clostridium difficile*. *PLoS*
540 *Genetics*, *9*(8), e1003660. https://doi.org/10.1371/journal.pgen.1003660
541 Fimlaid, K. A., Jensen, O., Donnelly, M. L., Francis, M. B., Sorg, J. A., & Shen, A. (2015).
542 Identification of a Novel Lipoprotein Regulator of *Clostridium difficile* Spore
543 Germination. *PLOS Pathogens*, *11*(10), e1005239.
544 https://doi.org/10.1371/journal.ppat.1005239
545 Galperin, M. Y., Mekhedov, S. L., Puigbo, P., Smirnov, S., Wolf, Y. I., & Rigden, D. J. (2012).
546 Genomic determinants of sporulation in Bacilli and Clostridia: Towards the minimal set
547 of sporulation-specific genes. *Environmental Microbiology*, *14*(11), 2870–2890.
548 https://doi.org/10.1111/j.1462-2920.2012.02841.x
549 Galperin, M. Y., Yutin, N., Wolf, Y. I., Vera Alvarez, R., & Koonin, E. V. (2022). Conservation
550 and Evolution of the Sporulation Gene Set in Diverse Members of the Firmicutes.
551 *Journal of Bacteriology*, *204*(6), e00079-22. https://doi.org/10.1128/jb.00079-22
552 Goffin, C., & Ghuysen, J.-M. (1998). Multimodular Penicillin-Binding Proteins: An Enigmatic
553 Family of Orthologs and Paralogs. *Microbiology and Molecular Biology Reviews*, *62*(4),
554 1079–1093.

555 Hartman, B. J., & Tomasz, A. (1984). Low-affinity penicillin-binding protein associated with
556 beta-lactam resistance in *Staphylococcus aureus*. *Journal of Bacteriology*, *158*(2), 513–
557 516. https://doi.org/10.1128/jb.158.2.513-516.1984
558 Henriques, A. O., de Lencastre, H., & Piggot, P. J. (1992). A *Bacillus subtilis* morphogene cluster
559 that includes *spoVE* is homologous to the mra region of *Escherichia coli*. *Biochimie*,
560 *74*(7–8), 735–748. https://doi.org/10.1016/0300-9084(92)90146-6
561 Isidro, J., Mendes, A. L., Serrano, M., O.Henriques, A., & Oleastro, M. (2017). Overview of
562 *Clostridium difficile* Infection: Life Cycle, Epidemiology, Antimicrobial Resistance and
563 Treatment. *Clostridium Difficile - A Comprehensive Overview*.
564 https://doi.org/10.5772/intechopen.69053
565 Isidro, J., Santos, A., Nunes, A., Borges, V., Silva, C., Vieira, L., Mendes, A. L., Serrano, M.,
566 Henriques, A. O., Gomes, J. P., & Oleastro, M. (2018). Imipenem Resistance in
567 *Clostridium difficile* Ribotype 017, Portugal. *Emerging Infectious Diseases*, *24*(4), 741–
568 745. https://doi.org/10.3201/eid2404.170095
569 Karimova, G., Pidoux, J., Ullmann, A., & Ladant, D. (1998). A bacterial two-hybrid system
570 based on a reconstituted signal transduction pathway. *Proceedings of the National*
571 *Academy of Sciences*, *95*(10), 5752–5756. https://doi.org/10.1073/pnas.95.10.5752
572 Katis, V. L., & Wake, R. G. (1999). Membrane-bound division proteins DivIB and DivIC of
573 *Bacillus subtilis* function solely through their external domains in both vegetative and
574 sporulation division. *Journal of Bacteriology*, *181*(9), 2710–2718.
575 https://doi.org/10.1128/JB.181.9.2710-2718.1999
576 Khanna, K., Lopez-Garrido, J., & Pogliano, K. (2020). Shaping an Endospore: Architectural
577 Transformations During *Bacillus subtilis* Sporulation. *Annual Review of Microbiology*,
578 *74*(1), 361–386. https://doi.org/10.1146/annurev-micro-022520-074650
579 Levin, P. A., & Losick, R. (1994). Characterization of a cell division gene from *Bacillus subtilis*
580 that is required for vegetative and sporulation septum formation. *Journal of Bacteriology*,
581 *176*(5), 1451–1459. https://doi.org/10.1128/jb.176.5.1451-1459.1994
582 Marmont, L. S., & Bernhardt, T. G. (2020). A conserved subcomplex within the bacterial
583 cytokinetic ring activates cell wall synthesis by the FtsW-FtsI synthase. *Proceedings of*
584 *the National Academy of Sciences*, *117*(38), 23879–23885.
585 https://doi.org/10.1073/pnas.2004598117

586 Meeske, A. J., Sham, L.-T., Kimsey, H., Koo, B.-M., Gross, C. A., Bernhardt, T. G., & Rudner,
587 D. Z. (2015). MurJ and a novel lipid II flippase are required for cell wall biogenesis in
588 *Bacillus subtilis*. *Proceedings of the National Academy of Sciences*, *112*(20), 6437–6442.
589 https://doi.org/10.1073/pnas.1504967112
590 Mitchell, S. L., Kearns, D. B., & Carlson, E. E. (2023). Penicillin-binding protein redundancy in
591 *Bacillus subtilis* enables growth during alkaline shock. *bioRxiv*, 2023.03.20.533529.
592 https://doi.org/10.1101/2023.03.20.533529
593 Mueller, E. A., Egan, A. J., Breukink, E., Vollmer, W., & Levin, P. A. (2019). Plasticity of
594 *Escherichia coli* cell wall metabolism promotes fitness and antibiotic resistance across
595 environmental conditions. *eLife*, *8*, e40754. https://doi.org/10.7554/eLife.40754
596 Nelson, M. E., Little, J. L., & Kristich, C. J. (2024). Pbp4 provides transpeptidase activity to the
597 FtsW-PbpB peptidoglycan synthase to drive cephalosporin resistance in *Enterococcus*
598 *faecalis*. *Antimicrobial Agents and Chemotherapy*, *68*(9), e00555-24.
599 https://doi.org/10.1128/aac.00555-24
600 Ng, Y. K., Ehsaan, M., Philip, S., Collery, M. M., Janoir, C., Collignon, A., Cartman, S. T., &
601 Minton, N. P. (2013). Expanding the Repertoire of Gene Tools for Precise Manipulation
602 of the *Clostridium difficile* Genome: Allelic Exchange Using pyrE Alleles. *PLOS ONE*,
603 *8*(2), e56051. https://doi.org/10.1371/journal.pone.0056051
604 Nonejuie, P., Burkart, M., Pogliano, K., & Pogliano, J. (2013). Bacterial cytological profiling
605 rapidly identifies the cellular pathways targeted by antibacterial molecules. *Proceedings*
606 *of the National Academy of Sciences*, *110*(40), 16169–16174.
607 https://doi.org/10.1073/pnas.1311066110
608 Pishdadian, K., Fimlaid, K. A., & Shen, A. (2015). SpoIIID-mediated regulation of σK function
609 during *Clostridium difficile* sporulation. *Molecular Microbiology*, *95*(2), 189–208.
610 https://doi.org/10.1111/mmi.12856
611 Pogliano, J., Osborne, N., Sharp, M. D., Abanes-De Mello, A., Perez, A., Sun, Y.-L., & Pogliano,
612 K. (1999). A vital stain for studying membrane dynamics in bacteria: A novel mechanism
613 controlling septation during *Bacillus subtilis* sporulation. *Molecular Microbiology*, *31*(4),
614 1149–1159. https://doi.org/10.1046/j.1365-2958.1999.01255.x

615 Rohs, P. D. A., & Bernhardt, T. G. (2021). Growth and Division of the Peptidoglycan Matrix.
616 *Annual Review of Microbiology*, *75*(1), 315–336. https://doi.org/10.1146/annurev-micro-
617 020518-120056
618 Sassine, J., Xu, M., Sidiq, K. R., Emmins, R., Errington, J., & Daniel, R. A. (2017). Functional
619 redundancy of division specific penicillin-binding proteins in *Bacillus subtilis*. *Molecular*
620 *Microbiology*, *106*(2), 304–318. https://doi.org/10.1111/mmi.13765
621 Saujet, L., Pereira, F. C., Serrano, M., Soutourina, O., Monot, M., Shelyakin, P. V., Gelfand, M.
622 S., Dupuy, B., Henriques, A. O., & Martin-Verstraete, I. (2013). Genome-wide analysis of
623 cell type-specific gene transcription during spore formation in *Clostridium difficile*. *PLoS*
624 *Genetics*, *9*(10), e1003756. https://doi.org/10.1371/journal.pgen.1003756
625 Sauvage, E., Kerff, F., Terrak, M., Ayala, J. A., & Charlier, P. (2008). The penicillin-binding
626 proteins: Structure and role in peptidoglycan biosynthesis. *FEMS Microbiology Reviews*,
627 *32*(2), 234–258. https://doi.org/10.1111/j.1574-6976.2008.00105.x
628 Schindelin, J., Arganda-Carreras, I., Frise, E., Kaynig, V., Longair, M., Pietzsch, T., Preibisch, S.,
629 Rueden, C., Saalfeld, S., Schmid, B., Tinevez, J.-Y., White, D. J., Hartenstein, V., Eliceiri,
630 K., Tomancak, P., & Cardona, A. (2012). Fiji: An open-source platform for biological-
631 image analysis. *Nature Methods*, *9*(7), Article 7. https://doi.org/10.1038/nmeth.2019
632 Shlosman, I., Fivenson, E. M., Gilman, M. S. A., Sisley, T. A., Walker, S., Bernhardt, T. G.,
633 Kruse, A. C., & Loparo, J. J. (2023). Allosteric activation of cell wall synthesis during
634 bacterial growth. *Nature Communications*, *14*(1), Article 1.
635 https://doi.org/10.1038/s41467-023-39037-9
636 Shrestha, S., Taib, N., Gribaldo, S., & Shen, A. (2023). Diversification of division mechanisms in
637 endospore-forming bacteria revealed by analyses of peptidoglycan synthesis in
638 *Clostridioides difficile*. *Nature Communications*, *14*(1), 7975.
639 https://doi.org/10.1038/s41467-023-43595-3
640 Sjodt, M., Rohs, P. D. A., Gilman, M. S. A., Erlandson, S. C., Zheng, S., Green, A. G., Brock, K.
641 P., Taguchi, A., Kahne, D., Walker, S., Marks, D. S., Rudner, D. Z., Bernhardt, T. G., &
642 Kruse, A. C. (2020). Structural coordination of polymerization and crosslinking by a
643 SEDS–bPBP peptidoglycan synthase complex. *Nature Microbiology*, *5*(6), Article 6.
644 https://doi.org/10.1038/s41564-020-0687-z

Srikhanta, Y. N., Hutton, M. L., Awad, M. M., Drinkwater, N., Singleton, J., Day, S. L., Cunningham, B. A., McGowan, S., & Lyras, D. (2019). Cephamycins inhibit pathogen sporulation and effectively treat recurrent *Clostridioides difficile* infection. *Nature Microbiology*, *4*(12), 2237–2245. https://doi.org/10.1038/s41564-019-0519-1

Taguchi, A., Welsh, M. A., Marmont, L. S., Lee, W., Sjodt, M., Kruse, A. C., Kahne, D., Bernhardt, T. G., & Walker, S. (2019). FtsW is a peptidoglycan polymerase that is functional only in complex with its cognate penicillin-binding protein. *Nature Microbiology*, *4*(4), Article 4. https://doi.org/10.1038/s41564-018-0345-x

Tan, I. S., & Ramamurthi, K. S. (2014). Spore formation in *Bacillus subtilis*. *Environmental Microbiology Reports*, *6*(3), 212–225. https://doi.org/10.1111/1758-2229.12130

Tsang, M.-J., & Bernhardt, T. G. (2015). A role for the FtsQLB complex in cytokinetic ring activation revealed by an *ftsL* allele that accelerates division. *Molecular Microbiology*, *95*(6), 925–944. https://doi.org/10.1111/mmi.12905

Wielders, C. L. C., Fluit, A. C., Brisse, S., Verhoef, J., & Schmitz, F. J. (2002). *mecA* Gene Is Widely Disseminated in *Staphylococcus aureus* Population. *Journal of Clinical Microbiology*, *40*(11), 3970–3975. https://doi.org/10.1128/JCM.40.11.3970-3975.2002

Yanouri, A., Daniel, R. A., Errington, J., & Buchanan, C. E. (1993). Cloning and sequencing of the cell division gene *pbpB*, which encodes penicillin-binding protein 2B in *Bacillus subtilis*. *Journal of Bacteriology*, *175*(23), 7604–7616. https://doi.org/10.1128/jb.175.23.7604-7616.1993

Zapun, A., Contreras-Martel, C., & Vernet, T. (2008). Penicillin-binding proteins and β-lactam resistance. *FEMS Microbiology Reviews*, *32*(2), 361–385. https://doi.org/10.1111/j.1574-6976.2007.00095.x